JOURNAL OF MATERIALS SCIENCE 35 (2000) 5057–5063

Formation and decay of a smectic mesophase during orientation of a PET/PEN copolymer

D. J. BLUNDELL, A. MAHENDRASINGAM*, C. MARTIN, W. FULLER
Department of Physics, Keele University, Staffordshire ST5 5BG, UK
E-mail: a.mahendrasingam@keele.ac.uk

An analysis has been made of time resolved wide angle X-ray scattering during the deformation of a 50%poly(ethylene terephthalate)/50%poly(ethylene 2,6naphthalate) copolymer at 120°C at a draw rate of the order of 10 s^{-1}. During the initial fast deformation a meridional reflection associated with a smectic mesophase is observed to form. After the initial deformation, the mesophase reflection decays at a rate of about 1 s^{-1}. During the decay, the lateral halfwidth of the meridional reflection increases indicating attrition of the smectic mesophase regions from the lateral interfaces. The sample deforms in a non-uniform manner. After the applied deformation ceases, the sample continues to thin down in the region of the X-ray beam. This is attributed to the lack of crystallisation during the 5 s timescale of observation. Analysis of the azimuthal profile of the strong inter-chain diffuse diffraction at ~2.8 nm^{-1} shows that the mesophase is associated with extended chains with a characteristic high alignment of segments along the deformation. During the period of decay of the mesophase it is proposed that the chain segments can be effectively divided into just two components: oriented mesophase and isotropic amorphous regions. The analysis indicates that the proportion of the mesophase varies from 80 to 40% during the observed decay period.

1. Introduction

The role of a mesophase structure as an intermediate state in the crystallisation of polymers was raised by Keller [1]. There is much current interest in this for both isotropic and oriented polymers [2–5]. We have recently reported a real time synchrotron study of the strain-induced crystallisation process during the orientation of poly(ethylene terephthalate) (PET) [6], in which a meridional reflection at ~1.0 nm^{-1} associated with a mesophase was seen to be created during drawing and was then transformed into the oriented crystalline phase. In a separate study, Welsh *et al*. [7, 8] have shown evidence of a smectic mesophase occurring as a transient state in the oriented crystallisation of a range of poly(ethylene terephthalate)/poly(ethylene 2,6naphthalate) (PET/PEN) copolymers. As part of their study, Welsh *et al*. report initial results of the real time synchrotron experiment to be described in this paper. In this experiment a film sample of a 50%PET/50%PEN copolymer was deformed over a period of about 1 second and then held at fixed overall length for a further 4 seconds. Diffraction corresponding to a smectic mesophase was observed during the initial deformation but decayed in intensity during the remainder of the experiment. This sample did not crystallise during the timescale of the experiment but was found to have crystallised after subsequent cooling. The detailed analysis of the data set of this 50%PET/50%PEN copolymer provides new information on the nature of the mesophase structure and on the changes that occur during the decay process.

Two diffraction features characterise PET/PEN mesophase structures in WAXS fibre patterns: a diffuse equatorial diffraction at around 2.8 nm^{-1} and a sharp meridional reflection at around 1.0 nm^{-1} related to the mean length of the monomer units. The equatorial feature is associated with the parallel alignment of chain segments along the fibre axis where the diffuse nature indicates that the segments are packed laterally in a liquid like manner. In the absence of the meridional feature this is consistent with a nematic arrangement of the monomer segments in which there is no lateral correlation between monomers in neighbouring chains. The added presence of the sharp meridional reflection with a narrow lateral width indicates that the segments occur as extended chains creating a periodicity related to the average length of a monomer. The lateral width of the meridonal suggests that there is a degree of register between monomers on adjacent chains. This type of order is consistent with a smectic mesophase structure. Since the mesogens consists of monomer units connected in a polymer chain, the mesophase can be more appropriately termed a chained smectic [9]. This type of register is distinct from the crystalline structures of the oriented homopolymers where the extended chain sequences are in a regular conformation and adjacent

* Author to whom all correspondence should be addressed.

chains are packed with three dimensional register on a triclinic lattice.

There have been several reports of a mesophase occurring in both oriented PET and PEN when prepared under specific conditions although only recently has there been evidence of the mesophase occurring as a transient state as a precursor to crystallization [6, 7]. Bonart [10] recognised both nematic and smectic states in a series of stretching experiments on PET and originally suggested that these mesophase states characterize stages in the crystallisation process. Later Bonart carried out cold drawing under various conditions and was able to produce all-nematic or all-smectic forms [11]. Asano and Seto [12] observed similar patterns in cold drawn and annealed fibres. Recently Asano *et al.* [13] have expanded the study on cold drawn PET that is subsequently annealed and demonstrated a progression from nematic to smectic and from smectic to crystalline order. Jakeways *et al.* [14] have reported a mesophase involving a sharp meridional reflection in PEN fibres prepared under particular conditions, although they did not assign the phase as smectic.

PET/PEN copolymers are of additional interest since their crystals have been shown to incorporate both monomers as Non Periodic Layer (NPL) crystals [15, 16]. These crystalline-like structures are analogous to those identified in thermotropic poly(hydroxy benzoic-hydroxy naphthoic acid) copolyesters [17]. Welsh *et al.* [7, 8] have proposed that the transient occurrence of an intermediate smectic state could explain the occurrence of a tilt of the resulting crystal chain axes away from the fibre axis in PET-rich copolymers in terms of a stress relieving mechanism. Asano *et al.* [13] have recently made a similar proposal for the tilt of PET homopolymer.

The 50%PET/50%PEN copolymer used in the synchrotron experiment is not easily crystallised from an isotropic melt state but can be crystallised as an NPL structure in oriented samples [15]. Although the copolymer did not actually crystallise during the period of the synchrotron observations, the observation of both the formation and the gradual decay of the smectic state provides new insight into the nature and stability of the transient mesophase structure. The analyses described in this paper combine measurements on the meridional diffraction with estimates of molecular orientation obtained from azimuthal scans of the diffuse equatorial diffraction. The results indicate that the smectic mesophase is uniquely associated with chain segments with a characteristic high orientation. There is evidence that the smectic regions are stress stabilised and resist attrition to isotropic configurations resulting from chain relaxation processes.

2. Experimental

The 50PET/50PEN mole% copolymer was supplied by W A MacDonald (Dupont Films) and was synthesised by a polycondensation reaction. Nuclear magnetic resonance analysis demonstrated that the copolymerisation was random. Amorphous films, 810 μm thick, were prepared by G Welsh [7, 8] by melt pressing at 170°C .

The *in situ* hot drawing, and wide angle X-ray diffraction experiments were performed on the microfocus beamline IDl3 at the European Synchrotron Radiation Facility (ESRF). The experiments used a purpose designed, X-ray diffraction camera constructed in the University of Keele Physics Department workshops [18]. The oven temperature could be controlled to within 1°C. A 10 mm wide sample was cut from the copolymer film and was clamped between two jaws attached to stepper motors which allowed uniaxial, bidirectional drawing.

The microfocus beamline on ID13 was configured to give a highly collimated beam with a diameter of approximately 30 μm at the specimen, with a wavelength of 0.092 nm . A minimum specimen to detector distance of 60 mm was available, at which d spacings out to 0.15 nm could be recorded. Diffraction patterns were recorded using a Photonics Science CCD detector, with a sensitive area 92 mm $\times$ 69 mm and an effective pixel area of 120 μm $\times$ 120 μm. Each diffraction pattern was recorded with an exposure time of 40 milliseconds. Over this period the pattern was integrated within the detector, before being digitised by a Synoptic i860 frame grabber. 124 frames were recorded sequentially with essentially no dead time between frames, thus providing a total observation period of 4.96 seconds with a time resolution of 40 milliseconds. The variation in size and shape of the specimen during drawing was recorded by the video recorder, also as a series of 40 milliseconds frames. The collection of the video recorder and X-ray diffraction frames was accurately synchronised. Ink reference stripes were drawn onto the films with a separation of 1 mm at right angles to the draw direction, to allow the draw ratio to be calculated from the video camera images. An alternative estimate of the change in draw ratio was obtained from the integrated intensity of each frame [19]. If it is assumed that the sample density remains constant during the draw and that the sample shape deforms in an affine manner then the thickness of the sample in the beam would be proportional to $1/\sqrt{\lambda}$. Thus the square of the inverse of the total intensity should be directly proportional to λ. This intensity relationship has the merit of monitoring the draw ratio at the part of the sample directly penetrated by the beam and is a better representation of precise drawing history when the sample deformation is non-uniform as in the present experiment. The image of the reference stripes provides confirmation of the draw ratio deduced from the intensity. The sample was mounted in the jaws of the camera with a 10 mm gauge length, heated to 120°C for 2 minutes and then drawn at a nominal draw rate of 12 s^{-1} for 0.24 seconds after which the jaws were held at fixed length. As a consequence of the yielding and relaxation characteristics of this sample, the deformation was non uniform and the sample continued to thin down in the region of the X-ray beam whilst the jaws were being held at fixed length. Using methods developed previously [19], every frame of the experiment was systematically analysed with a suite of macro programs in order to quantify the time evolution of the diffraction features associated with the mesophase.

Complete azimuthal circular scans were made at $\sim$2.8 nm^{-1} through the region of strong diffuse scattering in order to derive a profile associated with the

orientation distribution of the chain segments. It was assumed that the profile directly relates to the normals to the chain segments. The profiles were used to calculate the orientation order parameter $\langle P_2(\cos\theta)\rangle$ of the segments, where θ is the angle between the segment direction and the draw direction [20]. In doing this an assumption is made that the structure within the film sample retains uniaxial symmetry throughout the deformation. It is convenient to perform this calculation by first fitting the azimuthal profile to a Pearson 7[21] peak plus a level background and then calculating $\langle P_2(\cos\theta)\rangle$ from fitted parameters. This method artificially splits the chain segments into two populations, an isotropic component associated with the level background and a component where the segments are preferentially oriented around the deformation axis. The isotropic component has a $\langle P_2(\cos\theta)\rangle$ order parameter of zero and does not contribute to the deduced overall $\langle P_2(\cos\theta)\rangle$.

The lateral profile of the sharp meridional diffraction feature at $\sim$1.0 nm^{-1} was characterised by scanning the reflection with a horizontal slice and fitting the profile with a Pearson 7 peak. The peak height was divided by the integrated intensity of each frame in order to normalise the data to account for the thinning of the sample during the experiment. The area under the normalised fitted peaks can be used to follow the change in the integrated intensity of the meridional reflection for a given volume of sample. The pixel density was not sufficient to resolve changes in the profile of the reflection along the meridian direction.

3. Results

Fig. 1 shows representative diffraction frames and corresponding video images at different stages of the experiment. It should be noted that the tensile movement of the clamping jaws ceased during frame 6 where the local draw ratio is about 4 : 1. However the images of the sample show that, as a consequence of the yielding and stress relaxation characteristics deformation is non uniform and the sample continues to thin down

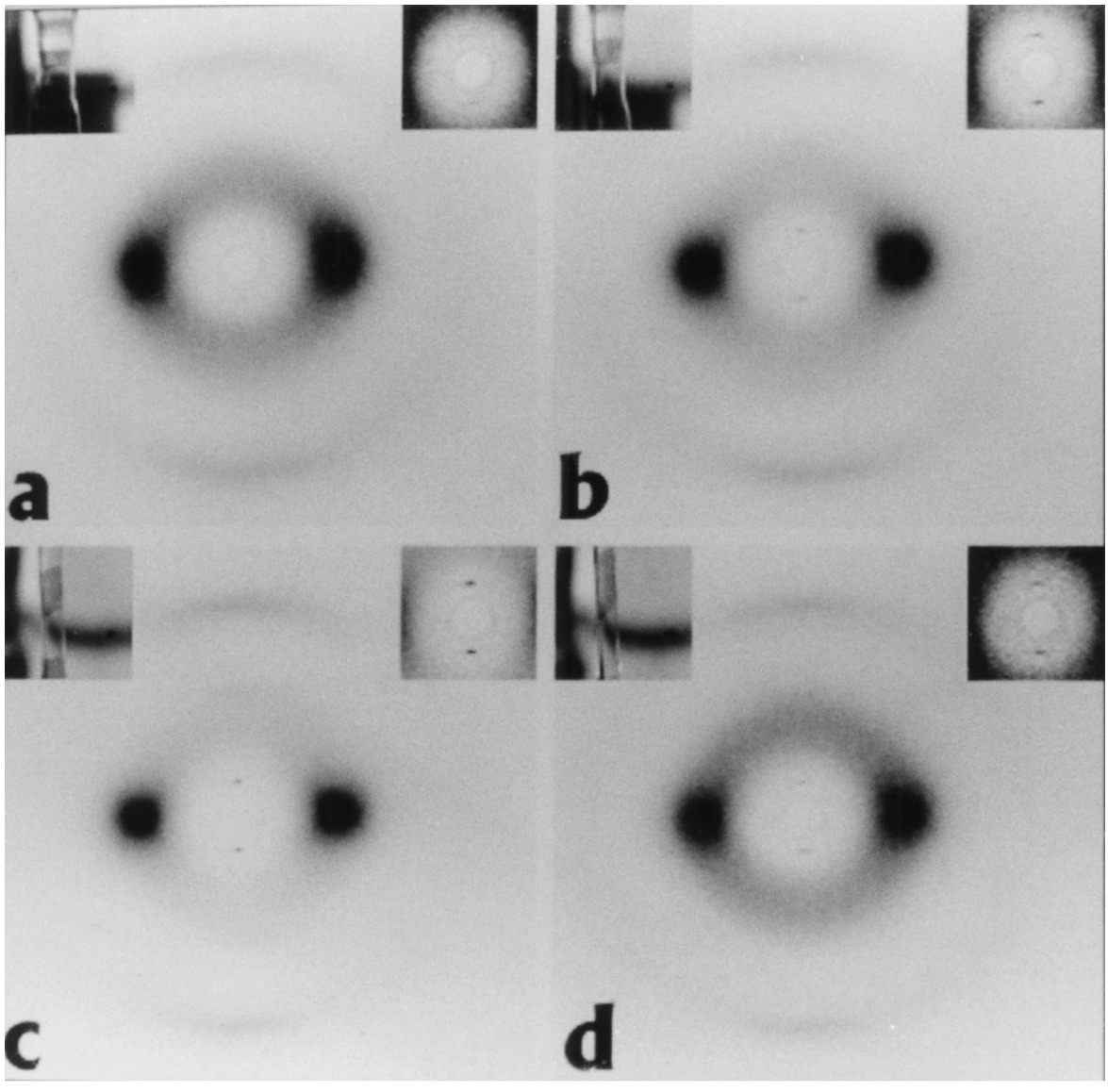

Figure 1 Selected X-ray diffraction patterns of a PET/PEN sample drawn at 120°C and draw rate 12.0 s^{-1}. Diffraction patterns (a–d) corresponding to frames **6** (0.24 seconds), **7** (0.28 seconds), **12** (0.48 seconds) and **124** (4.96 seconds). The corresponding video images of the sample are inserted in top left and the centre part of the diffraction showing the meridional reflection is inserted on top right of the figure.

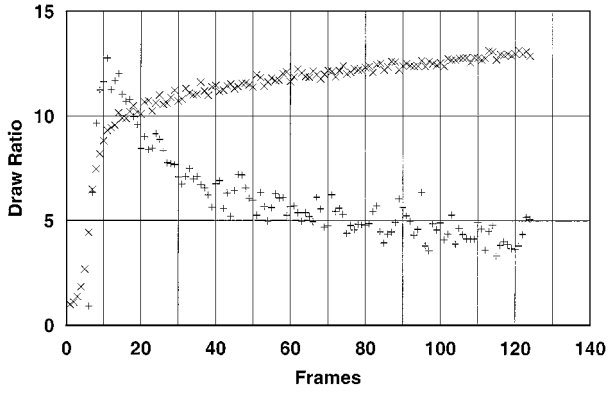

Figure 2 Plots showing the draw ratio derived from total intensity (×) and the integrated intensity of the meridional reflection for each frame in arbitrary unit (+). Each frame corresponds to 40 milliseconds.

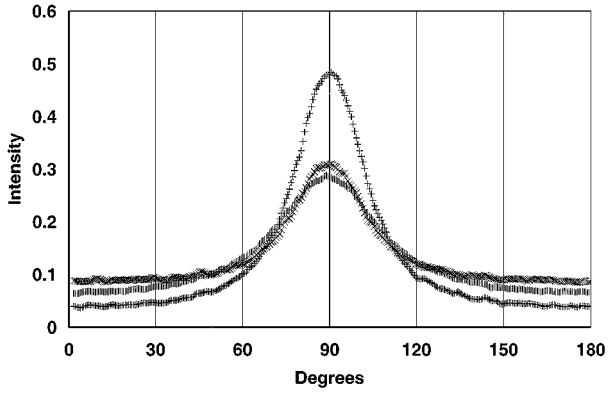

Figure 3 Azimuthal profiles at a scattering vector of 2.8 nm^{-1} for frames 6 (|), 12 (+) and 124 (×).

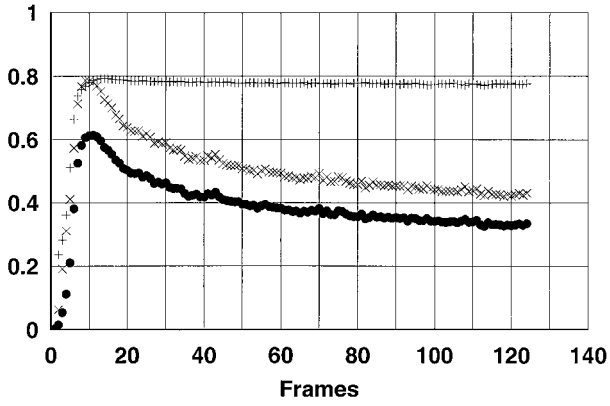

Figure 4 Plot of orientation order parameter $\langle P_2(\cos\theta)\rangle$ for each frame derived from the azimuthal profiles (•). Also shown are the weight fraction, w_A (×), and the order parameter, P_A (+) of the oriented component. Each frame corresponds to 40 milliseconds.

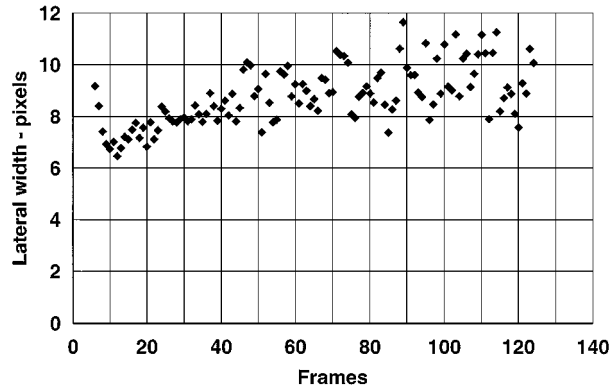

Figure 5 Half height width of the peak fitted to the lateral scan through the meridional reflection. Each frame corresponds to 40 milliseconds.

after the jaw movement has stopped. The local draw ratio deduced from the integrated intensity is plotted in Fig. 2 and shows that the deformation continues to increase at a similar rate beyond frame 6 up to frame 11 where the local draw ratio reaches about 9 : 1. The deformation rate then reduces but the draw ratio continues to increase for the rest of the experiment, reaching about 13 : 1 in frame 124.

Fig. 1 shows that up to frame 7 (0.28 s after the start of deformation), the intensity of the main diffuse halo becomes increasingly concentrated at the equator and thereafter retains a strong equatorial component. Examples of the azimuthal profiles of the diffuse halo at different stages are illustrated in Fig. 3. Up to around frame 12 (0.36 s) there is a gradual sharpening of the intensity around the equator above a level background. In the remaining frames there is an increase in the isotropic background level while the equatorial intensification decreases but remains with a similar azimuthal spread about the equatorial position. The overall $\langle P_2(\cos\theta)\rangle$ order parameter of all the chain segments deduced from these azimuthal profiles is plotted in Fig. 4 and shows that it reaches a maximum at around frame 10 (0.4 s).

The sharp meridional reflection first appears as a weak feature in frame 6 (0.24 s). It then intensifies in the next few frames up to around frame 12 (0.48 s) and thereafter appears to decrease in prominence. The integrated intensity of the meridional reflection normalised with respect to the total frame intensity is plotted together with the draw ratio in Fig. 2. There is a sharp rise in the intensity of the meridional up to frame 12 (0.48 s) corresponding to the period of deformation with a high rate of increase in draw ratio. This is followed by a marked fall off of intensity in the remaining frames with the intensity diminishing with a characteristic decay time of the order of one second. The maximum intensity of the meridional occurs at the frame close to where the $\langle P_2(\cos\theta)\rangle$ order parameter for the diffuse scattering at 2.8 nm^{-1} also goes through a maximum. The variation in the lateral halfwidth of the peak fitted to the meridional reflection is shown in Fig. 5. The increase in the scatter of the data with time is due to the reduced signal/noise resulting from the thinning of sample and broadening of the reflection. Up to frame 12 (0.48 s) there appears to be a slight decrease in halfwidth; thereafter there is a gradual increase in halfwidth over the period where the meridional reflection is decaying.

4. Discussion

The sharp meridional feature with a narrow lateral width combined with the concentrated equatorial diffraction is consistent with the presence of a smectic structure consisting of straight parallel chain sequences with liquid like spacing and with the segments of neighbouring chains having lateral correlation. Using higher definition diffraction patterns of a quenched sample of the same co-polymer, Welsh *et al.* [7, 8] have used the

Scherrer equation to estimate the lateral halfwidth of the meridional. This corresponds to a lateral extent of correlation in excess of 7 nm. The sharpness of this reflection in the meridional direction indicated the smectic regions have dimensions of 20 nm, or more, in the chain direction. Judging from the development of equatorial scatter at the time that the meridional develops, it is not possible to decide whether the smectic phase develops directly from the deformed network or whether it forms via a nematic phase, as suggested in the work of Bonart [10] and Asano *et al.* [13].

It is instructive to compare these results with our recent observations of a transient smectic mesophase in PET homopolymer when deformed at 90°C at a similar fast draw rate [19]. Up to a draw ratio of about 3 : 1 the $\langle P_2(\cos\theta)\rangle$ order parameter attains a similar level to that observed in the PET experiment indicating that the segments of the entangled chain network are responding in a similar way to the deformation. In the PET experiment, the mesophase developed quickly in the last stages of deformation up to the final draw ratio of 3.7 : 1. However unlike the present copolymer experiment, the oriented PET was found to start to crystallise as soon as the applied deformation ceased and there was no significant further extension of the sample after the onset of crystallisation. The crystals in the PET case can be considered as effective crosslinks that prevent chain retraction and rigidify the sample against further deformation. In the case of the present copolymer, no crystallisation occurs during the timescale of the experiment but the mesophase is seen to decay along with the continuing deformation. The continuing deformation of the sample after the crossheads have stopped indicates an ongoing relaxation which increases the compliance and enables part of the sample to extend further to relieve the applied stress. The decay of the smectic mesophase during this relaxation can be interpreted from two viewpoints, which are not necessarily conflicting. Either the cohesion of the chains in the smectic regions is significantly less than in a crystal and that this gives rise to a relaxation via a gradual breakdown of the parallel chain regions, or, the smectic mesophase is stabilised by the applied stress and that chain relaxation relieves the tension causing a loss of smectic structure. It is hoped to clarify the underlying causality of this relaxation with ongoing further experiments in which a simultaneous measurement of stress has been incorporated. It will be noted from Fig. 2 that the meridional reflection reaches a maximum at around frame 12, close to the end of the steep rise in draw ratio and then starts to decay as the rate of extension reduces. This is consistent with the fact that the decay of the mesophase commences when the extension rate reduces to the same magnitude as the mesophase decay rate ($\sim$1 s^{-1}). No information is available on the rates of the chain relaxation processes in this copolymer at 120°C but it is speculated that the decay is probably linked to a chain retraction process.

The increase in lateral halfwidth of the meridional reflection during the period of decay indicates a reduction in the lateral correlation or size of the smectic ordered regions. This suggests that part of the decay is due to attrition from the sides of the regions in which oriented chains breakaway and become disordered. However the rate of increase in halfwidth does not appear to fully account for the decay in overall peak intensity. This implies that the length of the extended configuration is probably also decreasing during the decay. Better resolution of the meridional reflection in the vertical direction will be needed to confirm this possibility.

The appearance of the smectic mesophase at a stage when the equatorial lobes reach a high prominence suggests that the artificial, two-component scheme used in the analysis of the azimuthal scans may have some meaning with respect to the structure and correlation of the chains. If one assumes a two component system for the orientation of the chain segments, where component A has an order parameter P_A and contributes a weight fraction w_A and where component B has an order parameter P_B, then the overall order parameter will be given by:-

$$\langle P_2(\cos\theta)\rangle = w_A P_A + (1 - w_A)P_B$$

If component B is associated with the isotropic component in the azimuthal analysis then:-

$$P_B = 0 \text{ and therefore } \langle P_2(\cos\theta)\rangle = w_A P_A.$$

The quantities P_A and w_A are, shown plotted along with $\langle P_2(\cos\theta)\rangle$ in Fig. 4. The plot shows that beyond frame 12 where the mesophase is fully established, the order parameter of the oriented component remains at a near constant 0.8 and that the decay in the overall $\langle P_2(\cos\theta)\rangle$ is in fact a consequence of a reduction in the amount of the oriented component rather than a fall in the degree of orientation of the component.

This behaviour suggests that it is worth exploring whether there is a direct quantitative link between the oriented equatorial diffraction and the mesophase meridional reflection. The observed intensity of the meridional reflection in the diffraction patterns represents a two dimensional cut through the sampled intensity function of the reflection in reciprocal space. In order to make a direct quantitative comparison it is necessary to compute the integrated intensity of the meridional reflection in reciprocal space by taking account of the lateral profile in the third dimension. If one assumes uniaxial symmetry, then the lateral width of the reflection in the third dimension will be identical to the lateral width in the observed diffraction pattern. Thus the variation of the integrated intensity function of the reflection in reciprocal space can be obtained by multiplying the observed integrated intensity by the lateral halfwidth. Fig. 6 shows a plot of the oriented component superimposed on a plot of the integrated intensity after suitable rescaling. The shapes of the two plots are remarkably similar and suggest that it might therefore be legitimate to associate the entire oriented component with the smectic mesophase.

In view of this very close correlation between the decay of the smectic meridional feature and the decay of the analytically fitted oriented component it is proposed that after about frame 12, the chain segments can be divided into just two components: a highly oriented

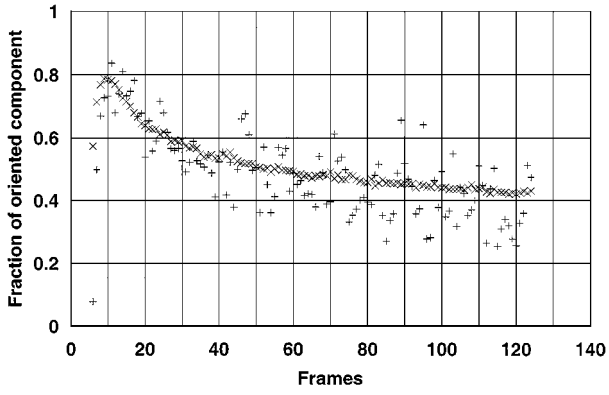

Figure 6 Fraction of oriented component w_A (×) overplotted with integrated meridional reflection (arbitrary unit) after a correction for uniaxial symmetry (+). Each frame corresponds to 40 milliseconds.

smectic component and a fully isotropic component. During the intitial deformation before frame 12 an additional oriented amorphous component is also expected to be present. The idea that the non-crystalline components of an oriented polymer can be split into two components is not in itself new. Lindner [22] devised a method for dividing the diffraction of PET fibres into three components consisting of a crystalline component and two non crystalline components, one of which he ascribed to a smectic mesophase since some of his samples exhibited the sharp meridional reflection. In Lindner's examples, both the amorphous and mesophase components were oriented. More recently Fu *et al.* [23] have carried out a sophisticated analysis of a highly crystalline PET fibre pattern in which the intensity is divided between highly oriented crystals, oriented amorphous and unoriented amorphous. However in their case, the samples did not show the features of a smectic mesophase. The proposed division between an oriented mesophase and an unoriented amorphous differs from these previous assignments. In this context it is instructive to compare frames 6 and 124, since both have a similar overall orientation with $\langle P_2(\cos\theta)\rangle = 0.38$ and 0.34 respectively but are composed of a different combination of non crystalline structure. Frame 6 is associated with the deformed network before any significant formation of a mesophase while frame 124 relates to a structure where a mesophase has been formed and has suffered a decay. As illustrated in the azimuthal profiles in Fig. 5, the oriented component in frame 124 is less pronounced but is sharper than in frame 6. This comparison of frames also emphasises the irreversible nature of the orientation during relaxation process. Once the mesophase has formed during the initial deformation, the following relaxation involves a reduction in the amount of oriented mesophase rather than a reverse of the original network orientation process. This situation is consistent with the mesophase being stress stabilised.

On the basis of this proposed two component interpretation, the results indicate that the smectic regions account for a very significant proportion of the total sample ranging from about 80% after the end of the initial fast strain rate and then falling to about 40% at the end of the observation period. The relatively low intensity of the meridional reflection, even when the smectic phase is at a maximum, indicates that the meridional structure factor associated with the smectic chain is extremely weak.

5. Conclusions

The entangled chain network of the 50%PET/50%PEN copolymer forms a smectic mesophase under similar deformation conditions to the previously observed transient smectic mesophase in PET homopolymer. Due to the slower crystallisation rate of the copolymer, crystals do not form quickly enough in order to stabilise and fix the chain orientation. Consequently after completion of the applied deformation there is a continuing relaxation which involves the decay of the smectic mesophase regions. The decay and relaxation occurs at a rate of the order of 1 s^{-1} and involves attrition of extended chains from the lateral surfaces of the smectic regions and probably also from the end faces.

The extended chain sequences involved in the smectic regions have a characteristic high alignment of segments along the deformation direction. During the decay of the mesophase, this high orientation is retained. The chains that are lost from the smectic mesophase quickly attain a random configuration so that during the decay the chain segments are effectively divided into only two components: isotropic random chain sequences or highly oriented smectic sequences. The proportion of the oriented component suggests the mesophase occupies about 80% of the sample at the end of the deformation and then decays to about 40% of the sample during the remainder of the experimental observations. The behaviour is consistent with the smectic mesophase being stress stabilised.

Acknowledgements

This work was supported by the allocation of beam time at the ESRF. We are grateful to M. Daniels, M. G. Davies, G. Dudley, E. J. T. Greasley, G. Marsh, M. Wallace and C. Sutton for technical support and help with preparation of the manuscript.

References

1. A. KELLER, NATO Advanced Research Workshop on Crystallisation of Polymers, Mons Belgium, 1992, edited by M. Dosier (Kluwer) p. 1.
2. M. IMAI, K. KAJI and T. KANAYA, *Macromolecules* **27** (1994) 7103.
3. N. J. TERRILL, J. P. A. FAIRCLOUGH, E. TOWNS-ANDREWS, B. U. KOMANSCHEK, R. J. YOUNG and A. J. RYAN, *Polymer* **39** (1998) 2381.
4. P. D. OLMSTED, W. C. K. POON, T. C. B. MCLEISH, N. J. TERRILL and A. J. RYAN, *Phys Rev Letters* **81** (1998) 373.
5. A. J. RYAN, J. P. A. FAIRCLOUGH, N. J. TERRILL, P. D. OLMSTED and W. C. K. POON, *Faraday Discuss.* **112** (1999) 13.
6. A. MAHENDRASINGAM, C. MARTIN, W. FULLER, D. J. BLUNDELL, R. J. OLDMAN, D. H. MACKERRON, J. L. HARVIE and C. RIEKEL, *Polymer* **41** (2000) 1217.
7. G. E. WELSH, D. J. BLUNDELL and A. H. WINDLE, *Macromolecules* **31** (1998) 7562.
8. *Idem.*, to be submitted.
9. A. H. WINDLE, in "Liquid Crystalline and Mesomorphic Polymers," edited by V. P. Shibaev and L. Lam (Springer, New York, 1994).
10. R. BONART, *Kolloid Z. Z.* **213** (1966) 1.

11. *Idem., ibid.* **231** (1968) 16.
12. T. ASANO and T. SETO, *Polymer Journal* **5** (1973) 72.
13. T. ASANO, F. J. BALTA CALLEJA, A. FLORES, M. TANIGAKI, M. F. MINA, C. SAWATARI, H. ITAGAKI, H. TAKAHASHI and I. HATTA, *Polymer* **40** (1999) 6475.
14. R. JAKEWAYS, J. L. KLEIN and I. M. WARD, *ibid.* **37** (1996) 3761.
15. X. LU and A. H. WINDLE, *ibid.* **36** (1995) 451.
16. *Idem., ibid.* 37 (1996) 2027.
17. S. HANNA and A. H. WINDLE, *ibid.* **29** (1988) 207.
18. A. MAHENDRASINGAM, W. FULLER, V. T. FORSYTH, R. J. OLDMAN, D. H. MACKERRON and D. J. BLUNDELL, *Rev. Sci. Instrum.* **63** (1992) 1087.
19. D. J. BLUNDELL, A. MAHENDRASINGAM, C. MARTIN, W. FULLER, D. H. MACKERRON, J. L. HARVIE, R. J. OLDMAN and C. RIEKEL, *Polymer*, in press.
20. R. LOVELL and G. R. MITCHELL, *Acta Cryst.* **37** (1981) 135.
21. M. M. HALL, V. G. VEERARAGHAVAN, H. RUBIN and P. G. WINCHELL, *J. Appl. Cryst.* **10** (1977) 66.
22. W. L. LINDNER, *Polymer* **14** (1973) 9.
23. Y. FU, W. R. BUSING, Y. JIN, K. AFFHOLTER and B. WUNDERLICH, *Macromolecular Chemistry and Physics* **195** (1994) 803.

Received 17 January
and accepted 16 February 2000